PAPER • **OPEN ACCESS**

Turbulent Flow in Annular Channels with Inner Tube Rotation a Calculated and Experimental Study

To cite this article: V A Zhigarev *et al* 2019 *IOP Conf. Ser.: Earth Environ. Sci.* **272** 022217

Turbulent Flow in Annular Channels with Inner Tube Rotation a Calculated and Experimental Study

V A Zhigarev[1], A V Minakov[1,2], E I Mikhienkova[1]

[1]Siberian Federal University, 79 Svobodny pr., Krasnoyarsk, 660041, Russia
[2]Institute of Thermophysics SB RAS, 1 Acad. Lavrentiev pr., Novosibirsk, 630090, Russia

E-mail: zhigarev.vladimir@yandex.ru

Abstract. A calculated and experimental study of the inner tube rotation effect on the pressure drop in the annular channel at the turbulent Newtonian flow was carried out. The Reynolds number varied from 2000 to 24000. The rotational Reynolds number ranged from 0 to 2100. The diameter ratio of the inner and outer pipes of the annular channel ranged from 0.286 to 0.714. Calculation was in good agreement with experiment.

1. Introduction

The main condition for the advance rise in mineral reserves to provide raw materials for industry and agriculture is the increase in the volume and quality of drilling operations. Development of drilling technologies is very important for exploration of all minerals kinds.

There have been significant changes in the exploration industry, in the creation of drilling equipment, advanced technologies, technological processes, and new types of rock-cutting tools in recent years. Fluid flows in the annular channels are found in many technical applications. The channels of heat exchangers, drilling columns, bearings, some kinds of mixers, etc. are an example of such structures. The flows features in annular channels with concentrically arranged cylindrical rotating surfaces are great practical interest. The flow of drilling fluid in oil wells, which described by an annular channel with a rotating inner tube, is the most common and important example of such flows. In most cases drilling muds are non-Newtonian viscoplastic fluids (such as Bingham plastics or pseudoplastics). This complicates the description of such flows.

A numerous theoretical and experimental material on fluid flows in the annular channels accumulated at present. A well-known analytical solution for Newtonian laminar flows in a concentric channel is in the textbook by Landau and Livshitz [1]. Analytical solution for the case of eccentric annular channels is unknown, however, many approximate and asymptotic solutions are proposed [2], including with the inner tube rotation. In addition there are quite a number of different empirical correlations for Newtonian flows operating in a particular range of parameters. The most common correlations are found in reference books [3-4].

It is necessary to highlight a series of experimental and calculated study [5-7] together with colleagues on the study of laminar and turbulent flows of Newtonian and non-Newtonian media in the annular channels with eccentricity and the inner tube rotation.

Despite the numerous number of theoretical, calculated and experimental studies on laminar and turbulent flows in the annular channel, the available material cannot provide the necessary information about all the flow in the required wide range of parameters of the drilling pipe and the rheological properties of the fluid, especially for non-Newtonian turbulent flow of drilling fluids in channels with eccentricity and of the inner pipe rotation. It is critical to have information about the hydraulic resistance and flow structure in the well during the drilling for effective and reliable control of the process. Therefore it is necessary a tool capable to predict these characteristics with good accuracy in a very wide range of parameters.

The purpose of this study was to create and verify an experimental setup and a numerical method for turbulent Newtonian flows in an annular channel with the inner tube rotation.

2. Experimental setup

An experimental setup was created to verify the numerical calculation of turbulent flows of Newtonian fluid in the annular channel (see figure 1). Measuring section simulated the well site. The setup was a closed circuit. Fluid from the tank (1) was supplied to the operating section by means of a centrifugal pump (2). The flow rate was regulated by the valves (3-4) and controlled by the flow meter (5). Then the fluid entered the operating section (6). The operating section was the annular channel of stainless steel, which was a system of "pipe in the pipe". The outer diameter of the inner pipe D_1=6; 10; 15 mm, the inner diameter of the outer pipe D_2=21 mm. Diameter ratio varied in the range from 0.286 to 0.714.

Pressure drop measurements on the measuring section of the annular channel were carried out using a differential pressure gauge (7). To measure the pressure drop in the outer pipe were installed fittings, to which a differential pressure gauge was connected. The inner pipe rotation was performed by means of a servo drive (8). The length of the measuring section was 0.5 m in the experiments. An input flow stabilization section was organized before the measuring section. In this study water was used as a working fluid. The fluid flow in the annular channel was varied in the range of 0.133 to 0.496 $kg \cdot s^{-1}$. This corresponded to the value of the Reynolds number from 2000 to 24000. The rotation frequency of the inner pipe varied from 0 to 5000 rpm.

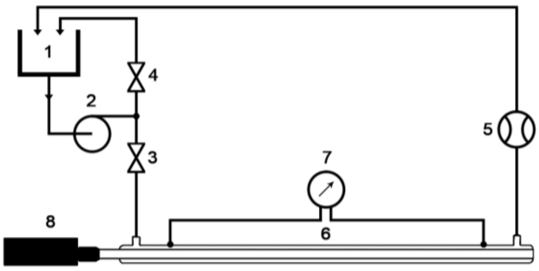

Figure 1. Schematic diagram of the experimental setup.

3. Mathematical model

A mathematical model of Newtonian turbulent flows in the annular channel with the inner pipe rotation was developed. The isothermal turbulent developed stationary incompressible fluid flow with constant density was considered. Both laminar and turbulent flows are usually described using the Navier-Stokes equation, but at present the capabilities of the computer technology allow the use of semi-empirical turbulence models using the Reynolds approach in the calculation of turbulent flows [8]. The essence of this approach is to solve the averaged Navier-Stokes equations:

$$\partial \rho \mathbf{v} / \partial t + \nabla (\rho \mathbf{v} \cdot \mathbf{v}) = -\nabla p + \nabla (\boldsymbol{\tau} - \rho \overline{\mathbf{v}' \cdot \mathbf{v}'}) + \mathbf{F}, \quad (1)$$

where $\boldsymbol{\tau}$ – time-averaged velocity field; $-\rho \overline{\mathbf{v}' \cdot \mathbf{v}'}$ – Reynolds stress tensor.

The Boussinesq hypothesis of isotropic turbulent viscosity is used in the construction of two-parameter turbulence models to determine the components of the Reynolds stress tensor:

$$-\rho \overline{\mathbf{v}' \cdot \mathbf{v}'} = \mu_t \left(\partial u_i / \partial x_j + \partial u_j / \partial x_i \right) - 2 \left(\rho k + \mu_t \, \partial u_i / \partial x_i \right) / 3 \delta_{ij} ,$$

where μ_t – turbulent viscosity; k – kinetic energy of turbulent fluctuations. A two-zone two-parameter model of SST mentor was used as the basic model for modeling turbulent flow in this paper [9].

The Menter model is written by a superposition of *k–ε* and *k–ω* models based on the fact that *k–ε* models better describe the properties of free shear flows, the *k–ω* models have an advantage in modeling the near-wall flows. A smooth transition from the k–*ω* model in the wall area to the *k–ε* model away from solid walls is provided by the introduction of the weight empirical function F_1. The second important detail of the model is to change the standard relationship between *k*, *ω* and the turbulent viscosity. Modification of this connection is the introduction of the transition to the Bradshaw equation in the near-wall region. The shear stress in the boundary layer is proportional to the energy of turbulent fluctuations according to the Bradshaw assumption.

Transport equations for *k* and *ω*:

$$\partial\rho k/\partial t + \nabla\left(\rho\mathbf{v}\cdot k\right) = \nabla\left((\mu - \sigma_k\mu_t)\cdot\nabla k\right) + \tilde{P} - \beta^*\rho\omega k, \quad (2)$$

$$\partial\rho\omega/\partial t + \nabla\left(\rho\mathbf{v}\cdot\omega\right) = \nabla\left((\mu + \sigma_\omega\mu_t)\cdot\nabla\omega\right) + \gamma\rho P/\mu_t - \beta\rho\omega^2 + \left(1 - F_1\right)\cdot\left(2\rho\sigma_{\omega 2}\left(1/\omega\right)\nabla k\cdot\nabla\omega\right).$$

A limiter is introduced in the turbulent energy generation term:

$$P = \boldsymbol{\tau}^t{}_{ij}\partial u_i/\partial x_j \quad \tilde{P} = \min\left(P, 20\cdot\beta^*\rho\omega k\right)$$

Weight function and its argument:

$$F_1 = \tanh(\arg^4{}_1),\ \ \arg_1 = \min(\max(k^{1/2}/\beta^*\omega y, 500\mu/\rho\omega y^2); 4\rho\sigma_{\omega 2}k/CD_{k\omega}y^2),$$

where the positive part of the cross diffusion terms in the transport equation ω:

$$CD_{k\omega} = \max(2\rho\sigma_{\omega 2}(1/\omega)\nabla k\cdot\nabla\omega; 10^{-10}),$$

Expressions for eddy viscosity due to hypothesis Bradshaw: $\mu_t = \rho a_1 k/\max(a_1\omega; F_2\Omega)$, where the vorticity value: $\Omega = \sqrt{2\Omega_{ij}\Omega_{ij}}$.

The switching function F_2 is defined as F_1:

$$F_2 = \tanh(\arg^2{}_2) \qquad \arg_2 = \max(2k^{1/2}/\beta^*\omega y, 500\mu/\rho\omega y^2).$$

Constants in transport equations are written by superposition of constants for the *k–ω* model and constants of the standard *k–ε* model.

The constants: $\phi = \phi_1 F_1 + \phi_2\left(1 - F_1\right)$, $\phi = \left\{\sigma_k, \sigma_\omega, \gamma, \beta\right\}$.

Set of constants for the wall layer of the SST model:

$$\sigma_{k1} = 0.85,\ \sigma_{\omega 1} = 0.5,\ \beta_1 = 0.075,\ \gamma = \beta_1/\beta^* - \sigma_{\omega 1}k^2/\sqrt{\beta^*}.$$

Set of constants for free-shear layers:

$$\sigma_{k2} = 1.0,\ \sigma_{\omega 2} = 0.856,\ \beta_2 = 0.0828,\ \gamma = \beta_2/\beta^* - \sigma_{\omega 2}k^2/\sqrt{\beta^*}.$$

Other constants used in the model: $\beta^* = 0.09,\ k = 0.41,\ a_1 = 0.31$.

The numerical method are detail described in [10-12]. Note the main features of the numerical method. The difference analogue of the convective-diffusion equations (1) – (2) is found using the finite volume method for unstructured grids. The approximation of convective terms of the transport equations is carried out by means of the second-order flow scheme QUICK respectively. Diffusion flows and source terms are approximated by finite-volume analogues of central-difference relations with second order of accuracy. The relationship between the fields of velocity and pressure, ensuring the fulfillment of the continuity equation, is implemented with the SIMPLEC procedure for combined grids. The difference equations obtained as a result of the discretization of the initial system of differential equations are solved iteratively using an algebraic multigrid solver.

4. Results and discussion

Figure 2 shows the contours and velocity profiles in the annular channel for different ratios of channel diameters.

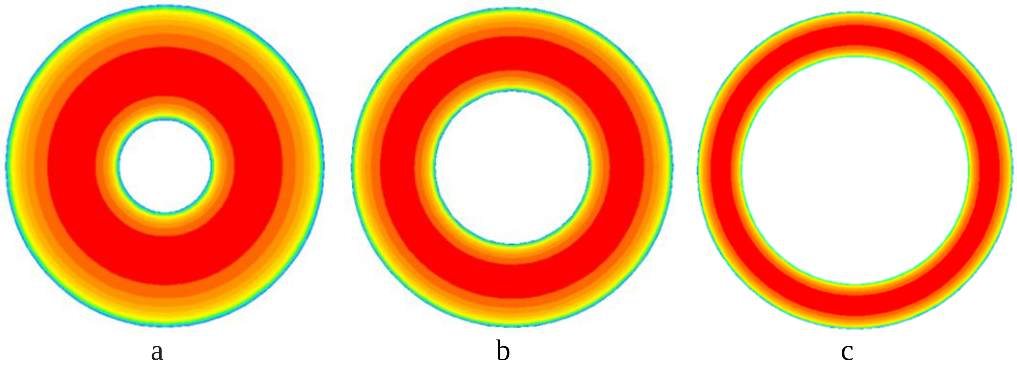

Figure 2. The contours of the velocity modulus in the annular channel for different diameters ratios without the inner pipe rotation for Q=0.496 kg·s^{-1}. a) D_1/D_2=0.286, b) D_1/D_2=0.476, c) D_1/D_2=0.714.

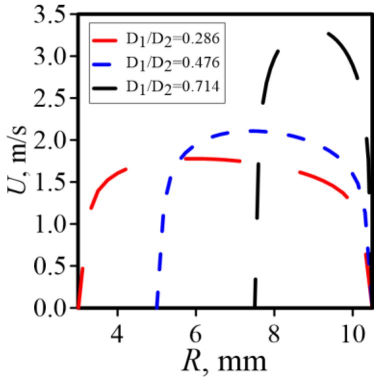

Figure 3. Profiles of the velocity axial component for different ratios of the pipes diameters without the inner pipe rotation.

The comparison of calculated and experimental values of the pressure drop in the considered annular channels is shown in figure 4. Analysis of the results shows that the calculation is consistent with the experimental data with an error not exceeding 5%. Figure 4 also presents data obtained by correlation [3-4].

The pressure drop in the annular channel is calculated as $\Delta P = \lambda L \rho U^2 / 2(D_2 - D_1)$, where $\lambda = 0.339/\mathrm{Re}^{0.25}$ is the coefficient of hydraulic resistance for turbulent conditions, L=0.5 m – length of the measuring section. The Reynolds number in the annular channel is defined as:

$$\mathrm{Re} = 4Q(D_2 - D_1)/\pi(D_2^2 - D_1^2)\mu .$$

The average flow rate in the annular channel is defined as $U = Q/\rho\pi(D_2^2 - D_1^2)$.
Evidently this correlation also well describes the experimental data and can be used to predict the pressure drop in turbulent Newtonian flow in annular channels without the inner tube rotation.

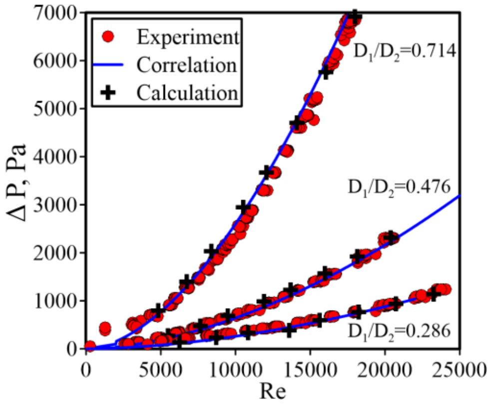

Figure 4. The pressure drop in the annular channel as function of the Reynolds number for different ratios of pipe diameters. The rotation velocity of the inner pipe is equal to 0.

The effect of the rotation velocity of the inner pipe on the value of the pressure drop in the annular channel is investigated further. Figure 5 shows the velocity profiles in the annular channel for two different rotations of the inner pipe. Abviously the maximum of the axial component of the velocity shifted towards the outer wall of the channel with the increase in the angular velocity of rotation of the inner tube. In addition the value of the tangential velocity in the center of the channel increased.

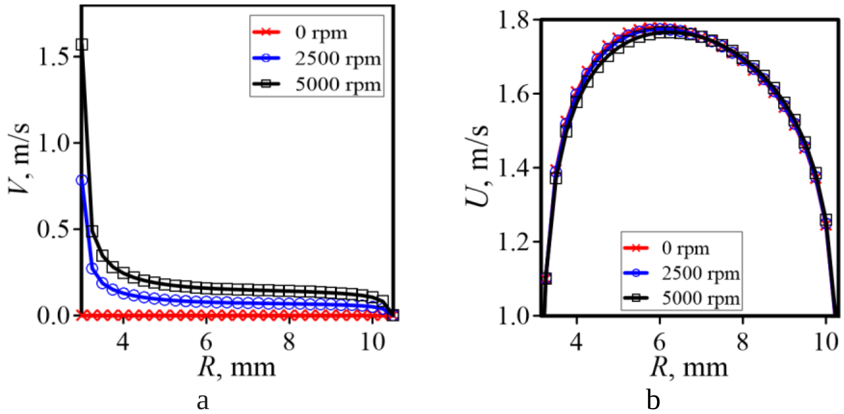

Figure 5. Profiles of the tangential (a) and axial (b) velocity components in the annular channel for different rotation velocities of the inner pipe at D_1/D_2=0.714.

The dependence of the pressure drop on the angular rotation velocity of the inner pipe for different values of the Reynolds number is shown in figure 6. The pressure drop in the annular channel increased with rising rotation velocity. The calculation showed satisfactory agreement with the experiment.

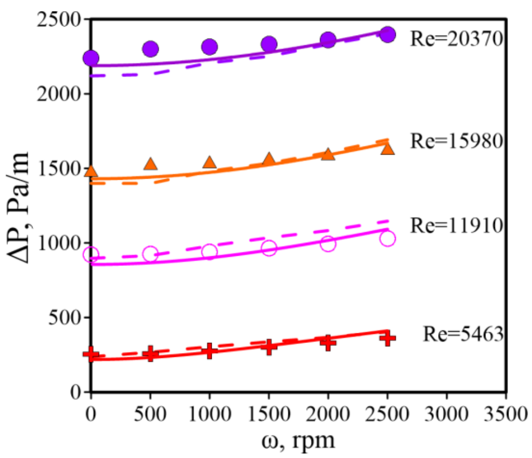

Figure 6. The pressure drop in the annular channel as function of the inner pipe rotation for different Reynolds numbers. Solid lines are correlation [15], dotted lines – calculation, points – experiment.

A comparison of this correlation with the calculation and experiment is shown in figure 6. The error in this case don't exceed 5%, which iss within the error of the experimental data.

The pressure drop in the annular channel as function of the inner pipe rotation for different Reynolds numbers. Solid lines are correlation [15], dotted lines - calculation, points - experiment.

There are several correlations [13-15] describing the effect of inner pipe rotation on the pressure drop in the annular channel at present. Analysis of calculated and experimental data showed that the following correlation best describes ones [15]:

$$\Delta P = \rho U^2 R_1 \lambda_s / 2(D_2 - D_1)$$

$$\lambda_s = (0.3354/2\mathrm{Re}_w^{0.25}) \cdot \left[\left[1 + 0.629(w \cdot R_1/U)^2\right]^{\frac{3}{8}} + \left[1 + 0.629(w \cdot R_1 \cdot \beta/U)^2\right]^{\frac{3}{8}} \right],$$

Parameter β is defined as $\beta = 0.1713\mathrm{Re}^{0.288} - 1.7e^{-10410/\mathrm{Re}_\omega}$, where $\mathrm{Re}_\omega = \rho R_1 \omega/\mu$ – rotational number.

5. Conclusion

An experimental setup for studying drilling mud flows in annular channels with different diameter ratios and the inner pipe rotation was created. A mathematical model of Newtonian turbulent flows in the annular channel with the inner pipe rotation was developed. The mathematical model was based on the *k-ω* SST RANS turbulence model. The calculation and experimental studies of the turbulent Newtonian flow in the annular channel were carried out. The results of calculation and experiment were compared with each other and with known empirical correlations. Satisfactory agreement of the results was obtained. The maximum discrepancy did not exceed 5% and was within the experimental error. This setup is planned to make a complexe study of non-Newtonian turbulent flows in the future.

6. References

[1] Landau L D and Lifshitz E M 1986 *Theoretical physics: Hydrodynamics* vol **10**(4) (Moscow:Nauka) p 736
[2] Snyder W T. and Gerald A 1965 *A.I.Ch.E. Journal* **11**(3) 462-467
[3] Kirillov P L 1984 *Handbook of thermohydraulic calculations* 1984 (Moscow:Energoatomizdat) p 296
[4] Idelchik I E 1992 *Handbook of hydraulic resistance* (Moscow: Mashinostroyeniye) p 672
[5] Escudier M P, Gouldson I W, Oliveira P J and Pinho F T 2000 *Int. J. Heat and Fluid Flow*. **21** 92–103
[6] Escudier M P, Oliveira P J, Pinho F T and Smith S 2002 *Exp. Fluids* **33** 101–111
[7] Nouri J M and Umur H 1993 *J. Fluid Mech.***253** 617-641
[8] Launder B E. 1972 *Lectures in mathematical models of turbulence* (London: Academic press)
[9] Menter F R 1994 *AIAA Journal*. **32**(8) 1598-1605
[10] Minakov A V, Rudyak V Y, Gavrilov A A and Dekterev A A 2012 *Thermophys. Aeromech.***19**(3) 385
[11] Minakov AV *Comput. Mathematics and Math. Phys.* **54**(10) 1560-70
[12] Minakov A V, Sentyabov A V, Platonov D V, Dekterev A A and Gavrilov A A 2015 *JPCS* **579**(1)
[13] Yamada Y 1962 *Bulletin of the JSME* **5**(18) 302-310
[14] Yamada Y, Nakabayashi K. and Maeda K 1969 *Bulletin of the JSME* **13**(53) 1032-40
[15] Nakashima C Y, Oliveira S J. and Caetano E F 2008 *Therm. Eng.* **7**(28-02) 27-34

Acknowledgments

The research was performed with the financial support of the Russian Science Foundation the project No. 17-79-20218.